Exploring the high pressure SEM

C. Mathieu [*,1], **L Khouchaf**[2] and **A Kadoun**[3]

[1]Université d'Artois, 62300 Lens , France
[2]Centre de Recherche de l'Ecole des Mines de Douai – BP 10838 – 59508 Douai – France
[3]Université de Sidi Bel Abbes – Sidi bel Abbes – 22000- Algérie

The high pressure SEM (HPSEM) is an important tool for materials characterisation. The presence of a gaseous atmosphere inside the specimen chamber permits to limit the charging effect and to obtain image with specific electron detector. The electron beam scattering due to the introduction of the gas within the specimen chamber of the HP-SEM influences the image quality and the microanalysis results. This paper describes the different electron detectors, the specific contrast in high-pressure conditions for non-conductive specimen and to interpret the x-ray microanalysis results.

Keywords Low vacuum SEM, Environmental SEM, Beam gas interactions, Contrast, Microanalysis

1. Introduction

Over the last 20 years, the environmental SEM (ESEM) and the variable pressure or low vacuum SEM, have gaining popularity as a viable tool for materials characterisation [1-3]. These two kinds of microscope permit to image with a high pressure in the specimen chamber non-conductive specimen without the need of conductive coating. It is more judicious to use the term of high pressure Scanning electron microscope (HPSEM) [4-5] to distinguish this SEM instrument family comparatively conventional high vacuum SEM. The high pressure Scanning electron microscope can be defined as a SEM instrument able to operate at several thousand Pa in its specimen chamber. Operation of this microscope follows similar conventions as high vacuum SEM's in that secondary electron (SE) and backscattered electrons (BSE) are generated at the sample surface. The presence of a gas generates also positive ions, which can be used to neutralize surface charge thereby facilitating the observation of non-conductive specimens. There exist various HPSEM designs but the basic principle is that the high vacuum in the electron column optics is separated from the high-pressure zone by differential pumping through a pressure limiting aperture (PLA). Various gases can be used (air, nitrogen, helium, water vapour) and the pressure range depends on the microscope model, some can go well above very high pressure allowing for the imaging of liquid whereas others reach a maximum pressure of 300 Pa. For the imaging of liquid the gas performs a thermodynamic role such as preventing the evaporation form the specimen.

The conventional Everhart - Thornley scintillation-photomultiplier secondary electron detector cannot function at elevated pressures due to the high voltage (+12 kV) involved in its operation. Indeed, the intense electric field cause the gas to break down at the pressure employed. As a result, SE imaging in the high pressure SEM has required the development of a new generation of SE detector that operate under high-pressure conditions.

The aims of this paper are to present successively the different electron detector in the low vacuum conditions and to examine the influence of the beam gas sample interactions for imaging the non-conductive specimen and to discuss the microanalysis specificity.

2. Imaging in high pressure condition

2.1 The backscattered detector

[*] Corresponding author: e-mail: christian.mathieu@univ-artois.fr, Phone: (33)321791782

Earlier, to overcome the problem of the break down of the gas, a solution [6] has been proposed to use a new backscattered electron detector in the high-pressure condition. Normally, we can expect that the backscattered electrons are non-sensitive to the surrounding area near the specimen and the resolution will not modified by the presence of the gas. As shown in figure 1, the image quality is decreased when the pressure of gas increases inside the specimen chamber. Between the vicinity of this aperture and the specimen surface, the electron beam profile is drastically modified. It has been found that due to the gas environment, the original beam is split into two fractions, unscattered and scattered electron fraction. The unscattered fraction retains the original electron distribution and the same diameter as the original electron probe, whilst the scatttered fraction forms a so –called electron skirt "beam skirt" and usually spreads beyond the size of the electron probe diameter.

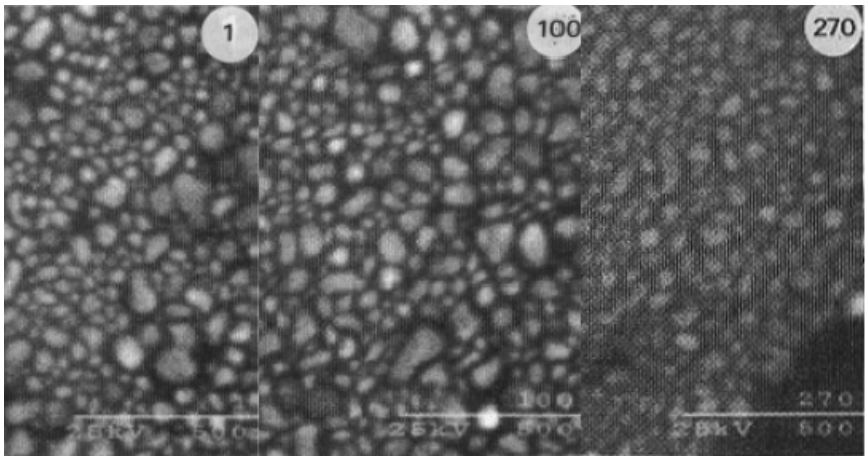

Fig. 1 A gold on carbon resolution standard imaged at 1, 100 and 270 Pa of air gas. In all cases, the accelerating voltage is equal to 25 kV with a working distance equal to 5 mm

Figure 1 show a series of gold on carbon resolution test imaged taken at 1, 100 and 270 Pa under air gas. Scattering in the gas induces a minor deterioration of the resolution and a correct image is obtained even at 270 Pa. The signal to noise ratio decreases and consequently the image quality decreases at high pressure. The scattered part of the electron beam in air conditions represents 20 % of the initial value [7]. Therefore, the emission of the backscattered electrons at the impact point is reduced while the interaction between the gas and the primary beam (and also the interaction between the backscattered electron with the gas) add a constant level of noise to the corresponding the useful signals from the specimen. Theoretical and experimental approaches have shown that the skirt effect is reduced if the gas has a low atomic number or a low effective number respectively for a gas or a molecule. Hence, several authors [8-13] have suggested to use the helium gas in order to minimize the beam skirt effect and to improve the image quality.

2.2. The secondary electron detector

The conventional Everhart –Thornley secondary electron detector cannot function due at elevated pressure. To overcome these limitations, three different ways have been used to measure the secondary electron signal in a high pressure SEM. In each approaches, a low voltage (< + 1000 V) positively biased electrode is placed near the pole piece (fig.2).

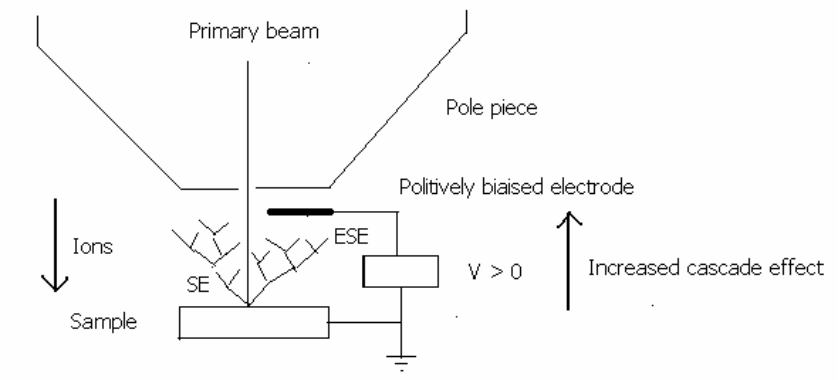

Fig 2 The accelerated SE collides with a gas molecule which ejects an ESE and leaves a positive ion behind. The SE and ESE accelerate in the field where more collisions occur. It is the amplification effect. The positive ions drift towards the sample surface

Secondary electrons emitted from the sample have energies of only a few electron volts and they are affected by the electric field in the chamber. The secondary electrons are accelerated towards the top of the chamber. When the kinetic energy exceed the ionisation threshold of the gas, an ionising collision can occur, creating a positive ion and an additional free electron called environmental secondary electron (ESE). Both electrons are then accelerated by the field and the process repeat, giving rise to a gas ionisation avalanche that amplifies the original emission signal. The positive ions are also affected by the electric field in the chamber. They drift towards the negatively charged sample surface. Ions are larger than electrons therefore they drift more slowly. When the positive ions collide with the sample surface, they recombine with the free electron surface thereby neutralizing the charge build – up. Moreover, the ionisation events modify the gas and light luminescence process can also occur.

Secondary electron images can be obtained by measuring the current induced in the positive electrode (the gaseous electron detector)[1,14-16], by measuring the current induced in the grounded stage (the ion current detector)[17-18] or by measuring the light emission from the gas via a photomultiplier (the gas luminescence detector). In all these detectors, it appears that comparatively to the backscattered electron detector, the beam gas interactions play an important role in the secondary electron detection by the amplification effect. This one depends on the type of the gas, the pressure, the electrode bias and the gas path length which is defined by the distance between the sample and the pressure-limiting aperture. Schematically, the signal to noise ratio increases when the ESE generation is favoured. Hence, ESE generation increases with pressure but there is a maximum. Increasing the pressure above this maximum decreases the production of ESE due to the presence of a space charge in the specimen chamber. Increasing the positive bias on the electrode increases the rate of acceleration and initiates more quickly. The number of ionization events increases exponentially as gas path length increases.

Concerning the Variation of the Resolution with the pressure, Thiel and al [19] have shown that the scattering in the gas results in only a minor deterioration of the resolution. So the skirt effect represents a minor inconvenience for imaging.

2.3 Other technology for SE detector

2.3.1 Two stage amplifier for ultrahigh resolution

Thiel and al have [20-21] developed a new detector for ultrahigh resolution imaging. An annular anode coaxial with the optic axis is used. The electric field is shaped by a grounded pressure limiting aperture situated above the anode and the sample surface situated below it. The electrode configuration was attached to the base of the objective lens of a field emission SEM equipped with an immersion lens

column. This one can be enhanced significantly the cascade gas amplification through the use of a magnetic field such as that provided by an immersion lens.

2.3.2 Differentially pumped secondary electron detector

In order to overcome the limitation of the Everhart Thornley detector in the high pressure SEM, an interesting solution has been proposed. The design of the E-T detector has been modified with a separated and differentially pumped detection chamber [22-23].

3. Contrast in high-pressure conditions

The field of application of the high pressure SEM for imaging is virtually unlimited (biological, metallurgical, mineral….). For many specimens, the interpretation of the electron contrast is quite similar that those obtained in high vacuum conditions. However, a new contrast called charge contrast imaging (CCI) is appeared for non-conductive specimen.[24-25]. This one is a highly complex, dynamic and transient phenomenon, thought to occur only in non-conductive sample imaged in the gaseous environment of high pressure SEM. Charge contrast images reveals structural informations, evident as contrast variations in the secondary electron image, which are not normally observed by conventional SEM imaging [26] (fig 3).

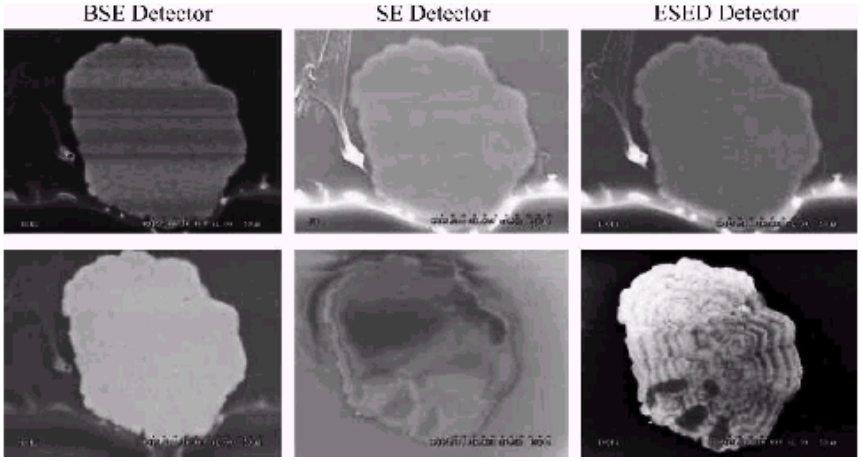

Fig 3 Comparison of the image ability of the BSE, SE and ion current detector (ESED) detectors on a gibbsite particle. The top row is the gibbsite with a conductive coating and the bottom layer is without. Microstructure is observed in the form of the growth rings on the uncoated gibbsite particle using the ESED.

CCI is related to charge trapping at the sample surface and it is associated with the gaseous environment and electron-ion-sample interactions. The complex theory behind how these unique variation contrast variation are generated is largely unknown but it has been the topic of discussion [26-27]
In practice, this novel imaging technique has the potential to provide data that are not evident by conventional imaging method. CCI has been used quite extensively to study geological minerals [25-26; 28] and polymeric materials [29]. This CCI has been recently shown for biomaterials [30].

4 X-ray microanalysis in high-pressure conditions

X-ray microanalysis in HP-SEM focuses on complication imposed by the skirt scattering and its effects on quantification. Several papers have presented the effect of the skirt on the x-ray microanalysis results [31-38].

In the particularly cases of non-conductive specimen, the insulators can develop either a positive or

negative surface potential under high-pressure conditions. It has been shown that the Duane hunt limit can be modified [39]. In this part, we studied the electron beam scattering due to the introduction of two gases : water vapour and helium within the specimen chamber of the HPSEM and the effects of this phenomenon on the image quality and on the microanalysis results.

4.1 unscattered fraction of the beam

In a simple mode of scattering where each point of the sample excited by scattered electrons, emits a signal proportional to the current of these electrons, the "unscattered fraction" of the electron beam can be written [2]:

$$\frac{I}{I_0} = \exp\left(-\frac{P \times L \times \sigma_t}{K \times T}\right)$$

I/Io : "unscattered fraction" of the electron beam
P : Pressure in the specimen chamber
L : Working distance (distance between the final aperture PLA1 and the surface of the sample)
σ_t : scattering cross section is specific to each gas molecule
K : Boltzman constant
T : Temperature in Kelvin

One can notice the exponential dependence of this fraction of the pressure, the nature of gas related to its scattering cross section (Tab.1) and of the working distance. During the experiments with the HPSEM, usually the pressure of the gas can vary in order to improve the quality of the image and to avoid the charging effect. In this work, we consider two gases: the water vapour (gas usually used in the ESEM) and helium. The experimental conditions are: an accelerating voltage of 20 kV and a working distance of 2 mm. On the table below (Tab.1) the scattering cross section of two gases used are given.

Table 1. Values of the total scattering cross section of various gases measured graphically at 20 kV [2].

Gas	Water vapour	Helium
Total scattering cross section (m^2)	2.10^{-21}	$0{,}25.10^{-21}$

Figure 4 shows the theoretical evolution of the calculated "unscattered fraction" of the electron beam according to the pressure in the water vapour and helium.

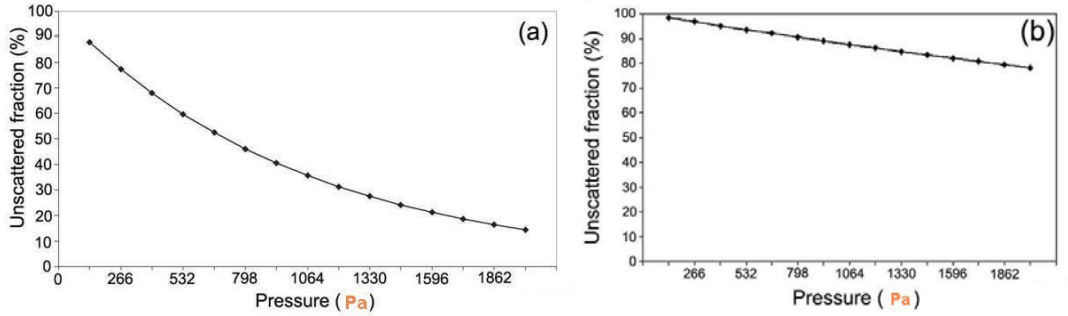

Fig 4. Evolution according to the pressure of the calculated "unscattered fraction" of the primary electron beam in two gases: (a) water vapour, (b) helium.

A clear difference between the evolution of this fraction in each case is observed. At 266 Pa (2 Torr), the unscattered fraction of this fraction is approximately 95 % for helium whereas it is 75 % in the water vapour. At 1330 Pa (10 Torr), this fraction represents more than 80 % of the total fraction in helium and is about 30 % in the water vapour. As we will show below, that behaviour will have obvious effects on the quality of the image and the results of microanalysis.

4.2 Effects in imagery

The images of an iron particle below show the influence of the beam skirt phenomenon on the imagery, under the same experimental conditions except the gas (Fig.5a and 5b). The experimental conditions used enabled us to work on rough samples without any preliminary preparation. The specimen is a silicon particle whose longest diameter is 160 μm containing iron particles on its surface in particular a small one at the center . This particle of 6 μm size is located at about 31-44 μm near the iron particles and about 40-50 μm near the carbon. This sample is a real situation that one encounters in microanalysis.

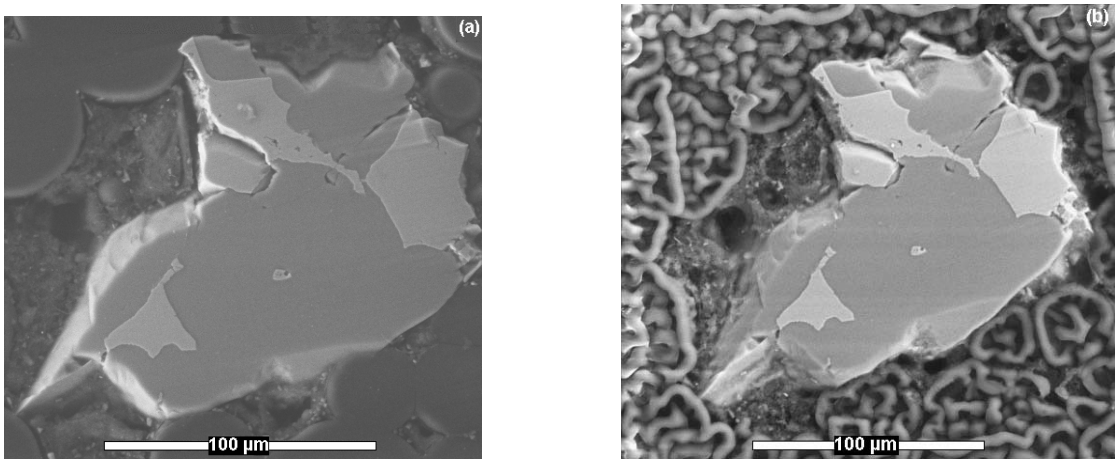

Fig 5. HPSEM micrographs with GSED detector of the sample at 2 Torr (266 Pa) and 20 kV in (a) water vapour, (b) helium.

A substantial improvement of the resolution and the quality of the image are obtained with helium due to a better focusing of the electron beam induced by an important "unscattered fraction" in comparison with water vapour. This phenomenon generates an increase in the signal-to-noise ratio inducing an improvement of the quality of the image. On the other hand, in helium, a degradation of the resin around the particle is observed. That represents a disadvantage of a better focusing of the electron beam with fragile materials such as the resin (polymeric). The use of low voltage and or low temperature can avoid this phenomenon

4.3 Effects in microanalysis X

In order to determine the effect of the interaction of the electron beam with gas on the results of microanalysis, we carried out the analysis of the particle in water vapour (gas usually used in the ESEM) and in helium. The goal of this experiment is also to validate the theoretical results obtained in paragraph 4.1. The beam is centered on the particle of 6μm. In order to avoid problems of instability of the electron beam, we chose times of acquisition short and refreshed the image between two acquisitions [37]. The pressure varies between 1 and 15 Torr (from 133 to 1995 Pa) with a step of 1 Torr. The evolution of the weight (%) obtained by using the emission lines Kα of iron, silicon, oxygen and carbon is presented in figure.6 below.

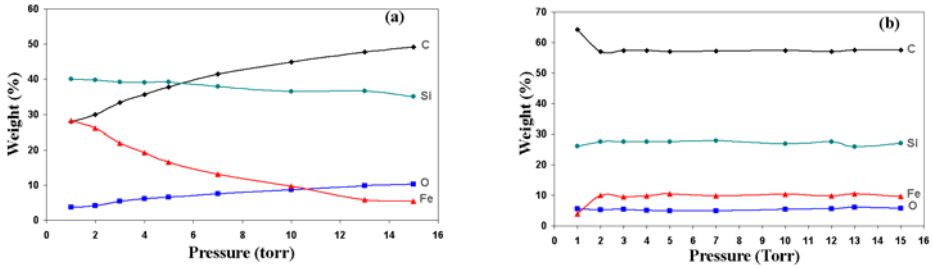

Fig 6. Evolution according to the pressure, of the microanalysis results of the different elements in a) water vapour, b) helium.

Since, we are interested in the analysis of the iron, a decrease in the percentage of iron with the increase of the water vapour pressure (Fig.6a) is observed which may attributed to the electron beam scattering phenomenon. In fact, when the pressure increases, the number of collisions between the primary electron beam and gas in the chamber increases and the number of electrons, which arrive on the iron particle, decrease. Indeed, it was shown [40], that for a pressure of 3 Torr (399 Pa), 45% of the primary electron beam is scattered beyond 25µm and 1,5% beyond 150µm for a working distance of 15mm and an accelerating voltage of 30 kV. Moreover, when the pressure reaches 5 Torr (665 Pa), 66% of the primary electron beam are scattered beyond 25µm and 8% beyond 150µm. Some authors, have suggested the use of the HPSEM under conditions very close to those of CSEM when operating microanalysis. The electron beam was focused on the iron particle placed at the center. We can obviously notice the very great stability of the results in comparison with those obtained in water vapour usually used in the specimen chamber of the ESEM and showing the good effect of the weak scattering of the electron beam when the gas used is the helium in agreement with the theoretical part showing the behaviour of the helium atoms used like gas. For example, for two pressure values of 2 and 10 Torr the weight of iron obtained between the two values of pressure in the helium is almost the same compared with the value obtained in the water vapour which varies considerably. This result shows how the results of microanalysis obtained in HPSEM can be affected by the problems caused by the electron beam scattering. In particular, when the gas used is water vapour (it is the case in all the ESEM). In addition, an instability of the results is observed for helium pressure lower than 2 Torr. Indeed, this phenomenon may be explained by the fact that the number of helium atoms is not yet sufficient to induce enough collisions, which give place to the creation of positive ions leading the neutralisation of the surface.

Conclusion

The High pressure SEM can be considered as an universal SEM. The presence of a gaseous atmosphere inside the specimen chamber permits to limit the charging effect and to obtain image with specific electron detector. A new contrast called charge contrast imaging (CCI) is appeared for non-conductive specimen in these particular conditions and the contrast origin must be investigated. The use of helium allowed an improvement of the chemical contrast and the quality of the images, and the stability of the results of microanalysis.

References

[1] G. D. Danilatos, Adv. Electron. Electron Phys **78**, 1 (1990)
[2] G. D. Danilatos, Adv. Electron. Electron Phys, **71**, 109 (1988)
[3] C. Mathieu Microscopy and Analysis, **43**,13 (1996)
[4] A. N. Farley, J. S. Shah, J. Microsc, **158**, 379 (1990)
[5] A. N. Farley, J. S. Shah, J. Microsc, **158,** 389 (1990)

[6] V. N. E. Robinson, J. Phys E Sci Instrum**, 8**,648(1975)
[7] C. Mathieu , Scanning Microscopy **13**, 23 (1999)
[8] S. J. Stowe, V.N.E Robinson Scanning, **20** 57 (1997)
[9] B. Adamiak, C Mathieu, Scanning, **22** 78 (2000)
[10] E. Oho,A. Akai, Sukehiro Itoh; Journal of electron Microscopy **49** , 761(2000)
[1I] A. Kadoun, R belkorissat,B khelifa, C Mathieu, Vacuum **69** 537 (2003)
[12] R. Belkorissat, A. Kadoun, B. Khelifa , C. Mathieu Micron**, 35** 543 (2004)
[13] L. Khouchaf**,** J. Verstraete, J. Phys IV **118** 237 (2004)
[14] P. Meredith, A.M.Donald, B. L. Thiel, Scanning, **18**, 467-473 (1996)
[15] A.L. Fletcher, B. L. Thiel, A.M.Donald, J. Phys. D Appl. Phys, **30**, 2249-2257 (1997)
[16] B. L. Thiel, I.C. Bache, A.L. Fletcher, P Meredith, A. M. Donald, J. Microsc, **187**,3, 143-157(1997)
[17] R. Durkin and J S Shah Journal of Microscopy, **1** 33 (1991)
[18] A. Mohan, N Khanna, J Hwu and D.C Joy, Scanning **20** 436(1998)
[19] B. L Thiel, M Toth, J Appl Phys **97**051101(2005)
[20] B. L Thiel, M Toth, P.M Schroemges, J.J. Scholtz,, G. Van Veen, W. R. Knowles, Rev Sci Instrum **77,** 033705 (2005)
[21] M. Toth, W. R . Knowles, B. L Thiel Appl Phys Lett **88**, 023105
[22] W Slowko Vacuum **63** 457 (2001)
[23] W. Slowko Vacuum **70** 157 (2003)
[24] B..J Griffin Microsc Microanal **3** 1197 (1997)
[25] B.J Griffin Scanning **22** 234 (2000)
[26] K. Robertson, R Gauvin, J Finch Mineral Engineering **18** 343 (2005)
[27] J. Cazaux Microsc Microa **10** 670 (2004)
[28] S.J. Cuthbert, J.O Buckman Am Mineral **90** 701 (2005)
[29] R. Gauvin, K Robertson, , J.F Leberre,J Finch, B. J Griffin Scanning **25** 240 (2003)
[30] P. L. Clode, Journal of Structural Biolology **155** 505 (2006)
[31] C. Mathieu Mikrochimica Acta[suppl], **15** 295 (1998)
[32] D.C.Sigee, C.Gilpin Scan microsc suppl, **15** 219 (1994)
[33] C. Gilpin, D.C.Sigee, J. Microsc**, 179** 22(1995)
[34] C. Mathieu Microscopy and Analysis, **60** 5 (1999)
[35] G.D. Danilatos, Mikrochimica Acta **114/115** 143 (1994)
[36] J.F. Mansfield, Mikrochimica Acta **132** 137 (2000)
[37] L. Khouchaf, J. Verstraete, J. Phys. IV. **12** 341 (2002)
[38] L. Khouchaf, F. Boinski, Vacuum **81** 599 (2007)
[39] X. Tang , D Joy Scanning **25** 194 (2003)
[40] B. Bolon, Microbeam. Anal., 199 (1991).